Distinct topological regimes in binary As_xSe_{1-x} glasses

1997 J. Phys.: Condens. Matter 9 9209

(http://iopscience.iop.org/0953-8984/9/43/007)

J. Phys.: Condens. Matter **9** (1997) 9209–9217. Printed in the UK PII: S0953-8984(97)81080-6

Distinct topological regimes in binary As_xSe_{1-x} glasses

V I Mikla

Institute for Solid State Physics and Chemistry, Uzhgorod State University, Voloshina Street 54, 294000 Uzhgorod, Ukraine

Received 20 January 1997, in final form 2 June 1997

Abstract. In the binary As_xSe_{1-x} glass system, a change of structural regime takes place near the composition $x \cong 0.04$. The presence of this topological threshold is established by direct and indirect evidence, such as peculiarities in the compositional dependence of the Raman vibrational modes, optical band-gap energy and drift mobilities of glasses. These peculiarities are caused by the transition from a chain–ring-like structure to chainlike structure.

1. Introduction

Over the past few years there has been an enormous effort to try to understand the properties of noncrystalline materials in terms of their microscopic structure. The loss of translational symmetry precludes the use of many conventional techniques. At the same time, a lack of translational regularity makes it possible to change continuously the elemental ratios in noncrystalline disordered compounds. Therefore, composition-dependent studies of physical properties seem to be very important for obtaining information about the structure of amorphous materials. Chalcogenide alloys are the best representatives of covalent glassy semiconductors. Owing to many applications in different fields, chalcogenide glasses are drawing a lot of attention [1, 2].

Composition-dependent studies on the physical properties of binary and ternary chalcogenide glasses give evidence for the existence of mechanical and chemical thresholds at certain compositions of these materials [3–5]. Of the glass-forming alloys of the group $A_x^V B_{1-x}^{VI}$, the As_xSe_{1-x} family is perhaps the most studied one, primarily because it is an exceptionally good glass former. The As–Se system displays main extrema of various properties at the stoichiometric composition (the mechanical and chemical thresholds coincides at $x = 0.40$). There seem to exist an additional threshold at $0.02 \leqslant x \leqslant 0.10$. It can be argued that the non-monotonic behaviour observed in the concentration dependence of glass-transition temperature, microhardness, density, etc [6, 7] in this range originates from changes in bonding topology.

In this paper, the change in the bond connectivity with the addition of As atoms to amorphous Se is studied by examining the compositional dependence of the structural and electronic properties. We find various signatures suggesting a structural change near $x = 0.04$, in addition to those at $x = 0.40$ and $x = 0.67$ predicted by Phillips [3] and Tanaka [5].

0953-8984/97/439209+09$19.50

2. Experimental details

The samples used were bulk glasses and amorphous films typically 5–50 μm thick. Bulk As_xSe_{1-x} glasses with $0 \leqslant x \leqslant 0.20$ were prepared by the usual melt quenching technique. To prepare a particular composition appropriate quantities of high-purity constituent elements, sealed in evacuated quartz ampoules (inner diameter 6 mm, wall thickness 0.8 mm, ampoule length 80 mm), were rotated continuously to ensure thorough mixing. The ampoules were then quenched in ice–water. Films of As_xSe_{1-x} glasses were prepared by vacuum evaporation. The amorphous nature of the films was confirmed by electron-probe microanalysis and Raman-scattering measurements. The compositions of the deposited films were determined by electron-probe microanalysis and the compositions quoted ($0 < x < 0.20$) are accurate to within 0.5 at.%. Annealing of the films was carried out in air at ambient pressure and at temperatures below the corresponding glass-transition temperature. After such a procedure their Raman spectra became indistinguishable from the corresponding spectra of melt-quenched glassy samples.

Optical transmission spectra of samples were measured and the transmittance was used to calculate the absorption coefficient.

We obtained the Raman scattering measurements using a right-angle scattering configuration. For illumination, we used the 647 nm line of an Ar^+ laser with the incident power kept below 10 mW cm^{-2} to prevent crystallization and photodarkening of the sample. We acquired the spectra using a RAMANOR-1000 spectrometer with photon counting electronics. The polarization of the incident light was parallel to the scattering plane. The details have been described elsewhere [8].

The photoelectronic properties were examined via time-of-flight (TOF), xerographic, and conventional (steady-state photocurrent) probes. All the measurements were performed at $T = 300$ K.

3. Results

3.1. Macroscopic characterization of glasses

First, we briefly review the behaviour of some fundamental physical properties. A simple way to characterize glasses is by their glass-transition temperatures, T_g, which can be observed as an endothermic process in differential scanning calorimetry. The results for the glass transition temperature are summarized in figure 1. The variation of T_g as a function of composition is linear with a change of slope at $x \sim 0.05$. This trend is in accordance with that observed by Borisova [7] and Mayers and Felty [6]. As a function of composition, microhardness exhibits a distinct maximum, and density a minimum, at ∼8 at.% As (figure 1). A minimum of DC conductivity and its pre-exponential term is observed in this region; for the activation energy E_σ some non-monotonicity is characteristic too.

3.2. Raman spectroscopy

Figure 2 displays typical spectra at selected x values. A cursory glance at these spectra reveals the relatively broad nature of the modes, indicating their glassy character. The effect of As alloying is to produce three noticeable changes in the spectrum of glassy selenium. First, the spectrum progressively broadens with x. In the As_xSe_{1-x} alloys, our second observation is that the low-frequency wing of the main maximum at 255 cm^{-1} qualitatively

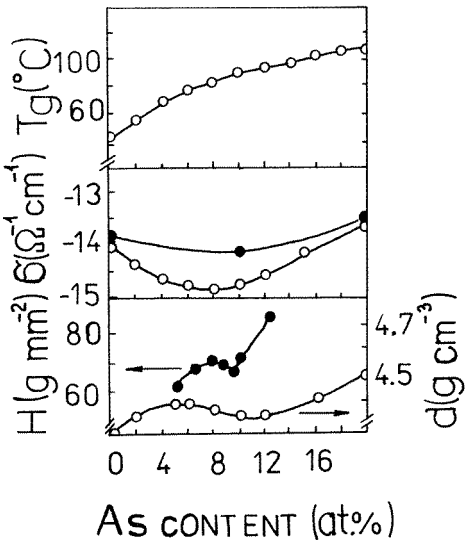

Figure 1. Glass transition temperature T_g (open circles—present data, solid line—data from [6]), density d, microhardness H [7], and room-temperature conductivity σ (open circles—present data, solid circles—data from [9]) for bulk glasses in the alloy system As_xSe_{1-x}.

increases in scattering strength and downshifts with x. It is necessary to note here that we associate the features in the region of the main vibration band, the 255 cm^{-1} peak and the 237 cm^{-1} shoulder, mainly with the chain vibrations. This assignment agrees with Raman data on the bulk and thin-film a-Se investigated recently [10–14]. Our third comment pertains to the region between 220 cm^{-1} and 230 cm^{-1} where we find the appearance of a broadened band, which is the most intense mode of the $As_{0.4}Se_{0.6}$ spectrum. The intensity of the 220 cm^{-1} band is almost constant up to $x = 0.04$. Then, at $x \sim 0.06$ an abrupt increase of the band intensity occurs. As the As content is further increased, a gradual intensity rise is observed for the band at 220 cm^{-1}. For $x > 0.35$ the band dominates the Raman spectrum.

The most significant aspect of the trends shown in figure 3 is the discontinuous character of the concentration dependence of the parameters A, ω_{max} and $\Delta\omega_{max}$. The parameter A represents the ratio of the integrated Raman intensity in the interval limited by the frequencies of $AsSe_{3/2}$ unit vibrations, 205 to 230 cm^{-1}, to the integrated intensity of valence vibrations. On the same figure, ω_{max} and $\Delta\omega_{max}$ represent the peak frequency and its full width at half maximum for difference spectra. These were obtained by subtracting the $As_{0.4}Se_{0.6}$ spectrum from As_xSe_{1-x} experimental spectra.

Another prominent spectral feature ascribed to ringlike segments [8, 10–14] is the weak, but strongly polarized mode at ∼112 cm^{-1}. The mode in question seen in pure Se diminishes with As addition and at ∼5 at.% As completely disappears. This is more vividly displayed in figure 4.

3.3. Total diffraction

All the compositions measured show a relatively well resolved diffraction peak at $Q(=4\pi \sin\theta/\lambda) \sim 1$–1.5 $Å^{-1}$, often termed the first sharp diffraction peak (FSDP),

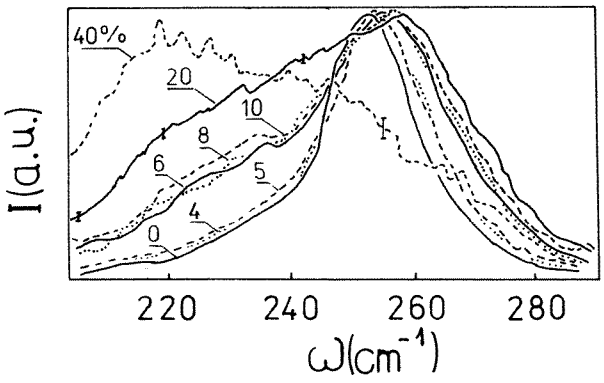

Figure 2. Compositional dependence of Raman spectra for a-As_xSe_{1-x} films. The respective values of x (in units of at.%) are indicated in the figure. The error bars show typical standard deviations.

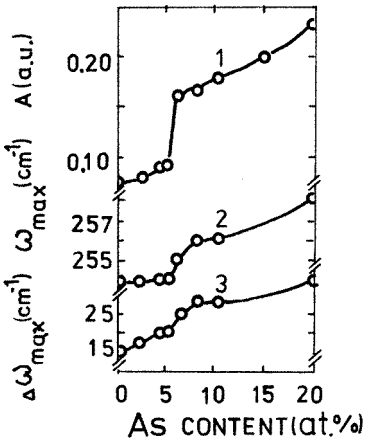

Figure 3. Composition dependence of the parameters A (1), ω_{max} (2) and $\Delta\omega_{max}$ (3) estimated from Raman spectra or from difference spectra.

indicative [15, 16] of appreciable medium-range order. The intensity and the position of the FSDP change with compositional variation. Figure 5 presents the compositional dependences of the intensity and the distance $d(=2\pi/Q)$ calculated from the FSDP for the amorphous As_xSe_{1-x} system. For comparative analysis the intensities are normalized with those of the second peak in the $I(Q)$ curve. We see that the intensity increases with arsenic content and peaks in the region $0.02 \leqslant x \leqslant 0.08$. The distance increases monotonically with x when $x \geqslant 0.08$.

3.4. Electronic properties

The variation of the measured optical band-gap energy E_0 as a function of composition parameter x in As_xSe_{1-x} alloys is shown in figure 6. It can be seen that the value of E_0 is close to that of amorphous Se for small As concentrations as expected and then it decreases as x increases. It has a minimum value at $x = 0.40$ which corresponds to the stoichiometric

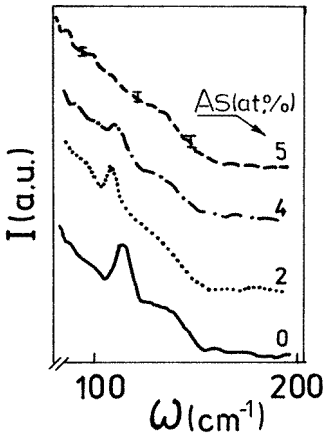

Figure 4. The bending mode region of the Raman spectra of a-As_xSe_{1-x} films. Each trace has been normalized to the height of the 255 cm^{-1} Raman band. The error bar shows typical standard deviations.

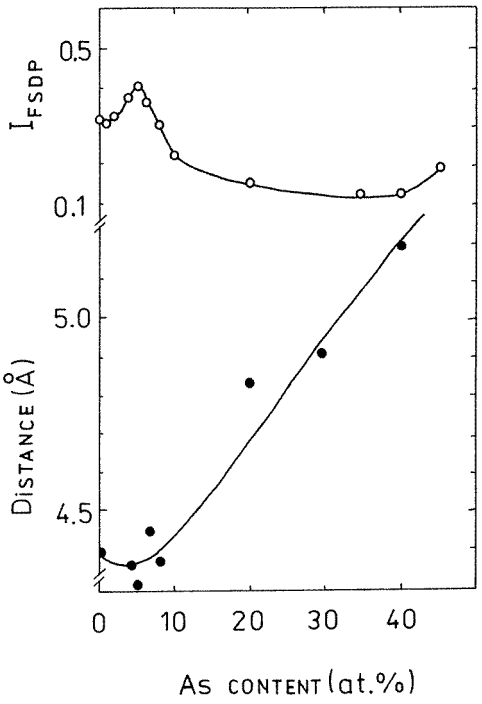

Figure 5. FSDP characteristics of a-As_xSe_{1-x} films as a function of composition. Open and solid symbols show the distance ($= 2\pi/Q$) and the normalized FSDP intensity I.

composition As_2Se_3. In addition to this extremum either a discontinuity or a rapid change occurs near $x = 0.04$.

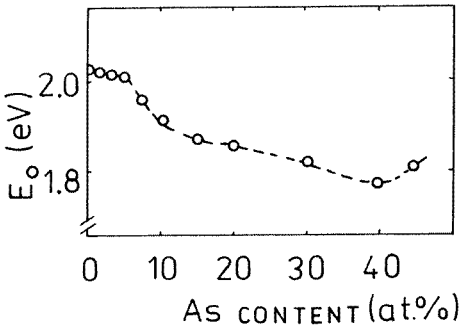

Figure 6. The optical band-gap energy E_0 for a-As_xSe_{1-x} films versus As concentration.

The data for the main electrophysical parameters of As_xSe_{1-x} alloys correlate with the compositional dependences of the structure. The DC conductivity reveals a smooth minimum for samples with $x = 0.06$. A similar dependence is seen for the conductivity activation energy. An increase in the pre-exponential factor of conductivity of the order of 1.5 in magnitude is also observed. The photosensitivity of As_xSe_{1-x} alloys has a similar compositional dependence. All the investigated parameters are in good agreement with the data [7, 9].

Amorphous As_xSe_{1-x} alloys with $0 \leqslant x \leqslant 0.20$ are particularly suitable for studying electron-transport properties because of their ambipolarity. The effect of progressive As addition on mobilities is illustrated in figure 7. Hole mobilities (solid circles), μ^h, and electron mobilities (open circles), μ^e, are plotted against at.% As in the alloy at $T = 300$ K. At low arsenic concentration ($x < 0.02$) the hole transit pulses are well defined and retain the shape they have in pure Se. For $0.02 \leqslant x \leqslant 0.06$, the hole response is absent. In this range it was not possible to detect any pulses associated with the transit of hole carriers. In accordance with extensive studies by Owen and Spear [17] and Schottmiller *et al* [18], only lifetime limited signals were observed for the case of photoinjected holes. Further progressive increase of As in the alloy drives the hole mobility down. The effect of As additions on the electron transport is less pronounced. We can distinguish two regions of exponentially decreasing dependence of electron mobility with increasing As content, as shown by the straight lines.

4. Discussion

In the following, we consider the changes occuring near $x = 0.04$ in the light of network-dimensionality considerations. The network dimensionality, D, is defined as the spatial dimension of covalently bonded clusters [3]. It is accepted [3–5] that $D = 1, 2$ or 3 for amorphous Se, As_2Se_3 or Si, respectively. $D = 1$, for instance, means chainlike morphology, in which entangled chain molecules are held together by weak van der Waals forces.

As we have shown, in the range of compositions investigated, many properties (physico-chemical, optical, electronic) of the As_xSe_{1-x} system change around $x = 0.04$ (a mean coordination number, z, of $\sim$2.04). The same behaviour is observed for vibrational properties. A possible explanation is that the above peculiarities are associated with the topological threshold which occurs when the chain–ring-like structure ($D \leqslant 1$) changes to a chainlike structure ($D \geqslant 1$).

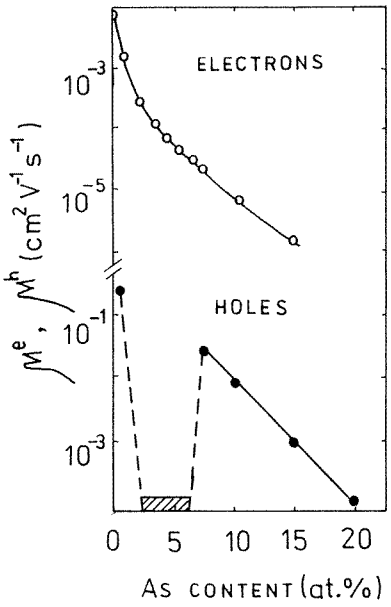

Figure 7. Drift mobilities of electrons and holes in a series of a-As_xSe_{1-x} films. T fixed at 300 K, $E = 100$ V μm^{-1}.

The structure of amorphous selenium has been the subject of many discussions in the literature. For a long time it was believed that the amorphous phase consists of rings and chains. However, recent structural studies on selenium and its alloys rather favour a random chain model, which assumes only local molecular order within a selenium chain (all atoms are in twofold coordinated chain structures and the dihedral angle is constant in magnitude but changes in sign randomly) [10, 14]. According to this model there are segments in a selenium chain characterized by repetition of the same dihedral angle ('chainlike' constituents) and segments characterized by alternating dihedral angles ('ringlike' constituents). Thus, we assume that in Se-rich glasses the network is dominated by Se atom chains (quasi-one-dimensional network) and addition of As atoms leads to branching owing to the threefold coordination of As atoms. The anomalous behaviour near $x = 0.04$ is ascribed to the disappearance of Se_8-like segments. From the point of view of configuration, it is suggested that the number of *cis*-configurations starts to decrease, so that the intermediate-range correlation is modified. The considerable reduction in the vibration mode at $\sim$112 cm^{-1} (figure 4), which is associated with *cis*-segments, strongly supports this suggestion. The Raman spectrum changes with composition, together with the estimated parameters ω_{max} and $\Delta\omega_{max}$ (see figures 2 and 3), allow us to conclude that incorporation of As leads to cross-links between chainlike or ringlike segments of a-Se.

There are strong indications that the compositional dependence of physico-chemical properties has no connection with chemical ordering. In fact, the binary As_xSe_{1-x} alloys exhibit extrema in the compositional dependence of the density not only at the $As_{0.4}Se_{0.6}$ composition, but also for the non-stoichiometric chalcogen-ring $As_{0.04}Se_{0.96}$ (shown in figure 1) and also for pnictogen-rich $As_{0.6}Se_{0.4}$ samples [7]. This means that the x dependence of the density originates from changes in bonding topology.

The origin of the FSDP has been studied extensively in recent years, but it remains controversial [5, 19, 20]. It has been shown that the FSDP has a similar appearance in glasses of different dimensionalities, for example in P_4Se_3, $SiSe_2$, $GeSe_2$ and SiO_2 whose crystalline analogues have dimensionality 0, 1, 2 and 3 respectively [20, 21]. The generally accepted idea is that the FSDP manifests the existence of some kind of medium-range structural correlation in amorphous networks. The assumption of a structural change at $x = 0.04$ gives a plausible explanation for the composition dependence of the FSDP shown in figure 5. Amorphous $As_{0.4}Se_{0.6}$ forms a two-dimensional network, and therefore it is conceivable that in the As_xSe_{1-x} system $D \leqslant 1$ when $x \leqslant 0.04$, $D \approx 1$ when $0.04 < x < 0.20$, and $D \approx 2$ otherwise. Hence, all a-As_xSe_{1-x} alloys with $x < 0.20$ appear to be essentially one dimensional. If this assertion is justified, the FSDP can be ascribed to the interchain correlation. Accordingly, the continuous intensity increase in the region $x < 0.04$ can be related to its evolution. At $x = 0.04$, the chain structure is fully developed, exhibiting the maximum FSDP intensity. In contrast, the decrease in the remaining part seems to indicate structural changes to more cross-linked networks.

The optical band-gap energy E_0 and related optical properties are determined mostly by the normal bonding configurations. In chalcogenide glasses, the conduction band arises from antibonding states and the valence band originates from the lone-pair-electron states. It appears that the conduction band broadens with x. This broadening is rather a consequence of short-range effects, accompanying the contraction of atomic volume. The bond energies of As–As, As–Se and Se–Se bonds are (2.07, 2.26 and 2.14 eV, respectively [22]) very close to one another. Therefore it is difficult to explain the observed variation of E_0 with x in the As_xSe_{1-x} system from the point of view of bond energy. On the basis of the above arguments, the composition dependence of the band-gap energy shown in figure 6 can be interpreted as follows. When x increases from zero, the band-gap energy slightly decreases predominantly through the short-range effect. Then, the continuous band-gap energy decrease in the region $x > 0.06$ can be associated with the enhancing degree of cross linking.

Electron transport in the amorphous As_xSe_{1-x} system is connected with the existence of ringlike constituents (*cis*-configurations) originally present in a-Se. Our Raman spectroscopic data show that the As additive decreases the population of the above constituent and it approaches zero for $x > 0.04$. The presence of two regions in the μ_e composition dependence (figure 7) indicates that besides the destruction of ringlike segments a development of some definite structural configuration becomes significant. This can be associated with the chain evolution and formation of cross-linked sites. In a-Se, the high concentration of traps at the discrete energy $\sim$0.29 eV above the valence band mobility edge control hole drift mobility as originally proposed by Spear [23]. Although these traps are known to be native defects (under- and over-coordinated charged structural defects), their exact nature has not been conclusively determined. Recently, Wong and coworkers [24] proposed that they may be due to dihedral angle distortions in the random structure of a-Se in which the lone pair orbitals on adjacent Se atoms approach parallel alignment. As apparent from the short lifetimes [17] and large xerographic residual potentials [25, 26] for As_xSe_{1-x} alloys with $x < 0.06$, the addition of As to a-Se seems to greatly increase the concentration of deep hole traps. They could be related to dangling ends of $=$As–Se–Se–Se–Se–Se–Se–Se–Se–Se$\cdot$ chains. These should occur as the Se_8 rings open up to connect to one As, but as the number of As is insufficient to allow closure. In the range of relatively low As concentration there is only a small number of the above structural defects and they are randomly dispersed through Se-host. Thus, these sites are structurally isolated and act as deep traps of extreme effectiveness, eliminating hole transport in the range $0.02 < x < 0.06$.

At higher As concentration ($x > 0.08$), a more continuous network begins to develop and the hole transit reappears.

5. Conclusions

There are a number of experimental indications of a critical composition at $x = 0.04$ in As_xSe_{1-x} glassy semiconductors. We suggest that the system probably undergoes a transition from $D < 1$, with an appreciable concentration of ringlike segments, to a chainlike structure with increasing degree of cross-linking.

References

[1] Madan A and Shaw P 1988 *The Physics and Applications of Amorphous Semiconductors* (New York: Academic)
[2] Tanaka K 1990 *Rev. Solid State Sci.* **2/3** 644
[3] Phillips J C 1981 *J. Non-Cryst. Solids* **43** 37
[4] Thorpe M F 1983 *J. Non-Cryst. Solids* **57** 355
[5] Tanaka K 1989 *Phys. Rev.* B **39** 1270
[6] Mayers M B and Felty E F 1967 *Mater. Res. Bull.* **2** 535
[7] Borisova Z U 1972 *Chemistry of Vitreous Semiconductors* (Leningrad: Izdatel'stuo Leningradsk. Univ.)
[8] Mikla V I, Baganich A A, Sokolov A P and Shebanin A P 1991 *Phys. Status Solidi* b **175** 281
[9] Hulls K and McMillan P W 1974 *J. Non-Cryst. Solids* **15** 357
[10] Lucovsky G 1980 *Proc. Int. Conf. on Phys. Selenium and Tellurium (1979)* (New York: Springer) p 178
[11] Brodsky M H and Cardona M 1978 *J. Non-Cryst. Solids* **31** 81
[12] Carroll P J and Lannin J S 1980 *J. Non-Cryst. Solids* **35–36** 1277
[13] Carroll P J and Lannin J S 1981 *Solid State Commun.* **40** 81
[14] Lucovsky G and Galeener F L 1980 *J. Non-Cryst. Solids* **35–36** 1209
[15] Phillips J C 1981 *J. Non-Cryst. Solids* **34** 153
[16] Luksha O V, Mikla V I, Ivanitsky V P, Mateleshko A V and Semak D G 1992 *J. Non-Cryst. Solids* **144** 253
[17] Owen A E and Spear W E 1976 *Phys. Chem. Glasses* **17** 174
[18] Schottmiller J, Tabak M, Lucovsky G and Ward A I 1970 *J. Non-Cryst. Solids* **4** 80
[19] Greaves G N, Elliott S R and Davis E A 1979 *Adv. Phys.* **28** 49
[20] Wright A C, Sinclair R N and Leadbetter A J 1985 *J. Non-Cryst. Solids* **71** 295
[21] Price D L, Susman S and Wright A C 1987 *J. Non-Cryst. Solids* **97–98** 167
[22] Rao K J and Mohan R 1981 *Solid State Commun.* **39** 1065
[23] Spear W E 1969 *J. Non-Cryst. Solids* **1** 197
[24] Wong C K, Lucovsky G and Bernholc J 1985 *J. Non-Cryst. Solids* **97–98** 1171
[25] Mikla V I, Semak D G, Mateleshko A V and Baganich A A 1990 *Phys. Status Solidi* a **117** 241
[26] Kasap S O 1991 *Handbook of Imaging Materials* (New York: Dekker) p 329